Journal of Alloys and Compounds 488 (2009) 533–537

Contents lists available at ScienceDirect

Journal of Alloys and Compounds

journal homepage: www.elsevier.com/locate/jallcom

Polymorphism in binary rare-earth metal germanides. Synthesis, structure and properties of the new hexagonal forms of Tb_3Ge_5 and Dy_3Ge_5

Paul H. Tobash[a], Svilen Bobev[a,*], Joe D. Thompson[b], John L. Sarrao[b]

[a] Department of Chemistry, University of Delaware, Newark, DE 19716, United States
[b] Materials Physics and Application Division (MPA-10), Los Alamos National Laboratory, Los Alamos, NM 87545, United States

ARTICLE INFO

Article history:
Received 12 May 2008
Received in revised form 7 October 2008
Accepted 14 October 2008
Available online 2 December 2008

Keywords:
Rare-earth germanides
Crystal structure
Polymorphism
Magnetic measurements
Tb_3Ge_5
Dy_3Ge_5

ABSTRACT

Reported are the synthesis, crystal structure determination and magnetic properties of new polymorphic forms of the rare-earth metal germanides Tb_3Ge_5 and Dy_3Ge_5. Both compounds are isostructural and crystallize with the hexagonal space group $P\bar{6}2c$ (No. 190, $Z = 2$) with unit-cell parameters $a = 6.861(2)$ Å; $c = 8.339(6)$ Å for Tb_3Ge_5 and $a = 6.8387(10)$ Å; $c = 8.293(2)$ Å for Dy_3Ge_5, respectively. The structures are derivatives of the ubiquitous AlB_2 type and can be regarded as its 6-fold superstructure ($a' = a \times 3^{1/2}$ and $c' = c \times 2$), arising from the long range ordering of Ge vacancies. They are therefore best described as flat Ge-layers, stacked in a hexagonal close-packed manner along the crystallographic *c*-axis, which are separated by layers of rare-earth metal atoms. Magnetic susceptibility measurements reveal that both Tb_3Ge_5 and Dy_3Ge_5 exhibit antiferromagnetic order at temperatures below 23 K and 9 K, respectively.

1. Introduction

Rare-earth metal (*RE* hereafter) germanides are intermetallic compounds, whose structures feature copious bonding patterns [1–3]. This is particularly true for the digermanides, many of which were originally thought to be fully stoichiometric $REGe_2$ binary phases crystallizing with the ubiquitous AlB_2 and α-$ThSi_2$ structure types [3]. However, this rarely holds true and almost exclusively, non-stoichiometric $REGe_{2-x}$ compounds are formed ($0 \le x \le 0.5$) [4–12]. Our recent efforts in exploring this rich structural chemistry have been facilitated through the use of the metal flux method [13] for the synthesis and the crystal growth of several new binary and ternary compounds [4–6,14–18]. On one extreme, we have demonstrated the reactive nature of the metal flux, as evidenced from the formation of the ternary compounds RE_2InGe_2 (*RE* = Sm, Gd–Ho, Yb) [14] and $RESn_{1+x}Ge_{1-x}$ (*RE* = Y, Gd–Tm) [16]. On the other side, owing to its function as a solvent, the metal-flux has played a beneficial role in our attempts to synthesize the new Gd_3Ge_4 [6] and RE_3Ge_5 compounds (*RE* = Sm, Gd) [4] or the metastable polymorph of the alkaline-earth phase $CaGe_2$ [18]. Herein, we exploit again the utility of the flux method for structural studies within a few more *RE*–Ge binary systems and present the synthesis of two new hexagonal polymorphs of the binary compounds Tb_3Ge_5 and Dy_3Ge_5, referred hereafter to as their β-forms (the known orthorhombic polymorphs of Tb_3Ge_5 [19] and Dy_3Ge_5 [20] are designated as the α-forms, respectively). Crystals have been grown from their respective elements using In flux, and their structures elucidated from single-crystal X-ray diffraction. Both compounds crystallize in the hexagonal Sm_3Ge_5 type [4] with the space group $P\bar{6}2c$ (Pearson's symbol *hP*16). Along with the structural relationship to the AlB_2 type [3], brought about through a long range ordering of vacant Ge sites, discussed as well are the temperature-dependent magnetization measurements on both compounds and a short description of the structural trends across the series.

2. Experimental

2.1. Synthesis

The reactants were pure elements from Alfa (purity > 99.9% metal basis), which were used as received. They were stored and handled inside an argon-filled glovebox with controlled oxygen and moisture levels below 1 ppm or under vacuum. The reaction conditions were identical to those used for the synthesis of the recently reported Sm_3Ge_5 and Gd_3Ge_5 [4]. Stoichiometric mixtures of the elements in a ratio of *RE*:Ge:In = 3:5:30 were loaded in alumina crucibles (Coors®, 2 cm^3), which were encapsulated in fused silica ampoules. The ampoules were evacuated (*ca.* 10^{-3} Torr) and flame-sealed. The reactions took place in muffle furnaces at 1373 K for 3 h, followed by a cooling step (rate 30°/h) to 773 K, where the flux was removed as described in detail previously [14]. Upon opening the sealed tubes, needle-like

* Corresponding author at: Department of Chemistry and Biochemistry, University of Delaware, Newark, DE 19716, United States. Tel.: +1 302 831 8720; fax: +1 302 831 6335.
E-mail address: bobev@udel.edu (S. Bobev).

0925-8388/$ – see front matter
doi:10.1016/j.jallcom.2008.10.046

crystals were isolated and later characterized by single-crystal and powder X-ray diffraction as being new hexagonal polymorphs of the known compounds Tb_3Ge_5 [19] and Dy_3Ge_5 [20]. Other metal fluxes were also explored – Cd and Pb for example worked as well – but the quality of the grown crystals was inferior. The crystals of Tb_3Ge_5 and Dy_3Ge_5 exhibit a silver-metallic luster and appear air- and moisture-stable over periods of time greater than 1 year.

It was initially found [4], and confirmed by this study, that the cooling rate in the aforementioned flux reactions is of particular importance with regard to the formation of either RE_3Ge_5 polymorph—cooling at slower rates (*e.g.* 5–10°/h) leads to the formation of the orthorhombic phase, while faster cooling (above) yields the hexagonal phase. This could be understood if one realizes that in molten In (or another suitable metal flux), the rates of nucleation and crystallization are under kinetic control and that upon slow cooling, the slower growing α-RE_3Ge_5 will be the major product; fast cooling will yield the faster growing β-RE_3Ge_5 polymorph as a majority phase. These observations, combined with the fact that polycrystalline samples of β-Tb_3Ge_5 and β-Dy_3Ge_5 could not be made by arc-melting and annealing are suggestive of β-polymorphs being metastable, kinetic phases, whereas the α-forms are the thermodynamically stable phases at ambient pressure and temperature. This conclusion is further corroborated by the irreversible single-crystal to single-crystal phase transition, discussed later on, and confirmed by the exclusive formation of the α-polymorphs by direct fusion of the corresponding elements.

2.2. X-ray diffraction studies

X-ray powder diffraction patterns were taken at room temperature on a Rigaku MiniFlex powder diffractometer using filtered Cu Kα radiation. The typical scans were in θ–θ mode ($2\theta_{max}$ = 80°) with a step-size of 0.05° and 10 s/step counting time. The collected powder patterns were used for phase identification only. This was done using the JADE 6.5 software package [21]. The intensities and the positions of the experimental and the calculated from the crystal structures peaks were in excellent agreement.

Single-crystal data collections were carried out on a Bruker SMART CCD diffractometer using monochromated Mo Kα radiation. The crystals were mounted on glass fibers with the aid of Paratone-N oil, which required the use of cryogenic temperatures (120 K in this case) in order for the viscous liquid to freeze and prevent the crystals from moving during the data collection. Full spheres of intensity data for crystals from both compounds were collected in 4 batch runs at different ω and ϕ angles. Data collections were handled in a routine fashion using the SMART software; the collected frames were integrated using the SAINTplus program [22]. The latter was also used for global unit cell refinement taking into account all reflections. Semi-empirical absorption correction based on equivalents was applied with SADABS [23]. The structures were refined on F^2 using the SHELX package; the coordinates from the isostructural Sm_3Ge_5 [4] were used as the starting model. In the last refinement cycles, all atomic positions were refined with anisotropic displacement parameters, leading to quick convergences and excellent goodness of fit. Final residuals and other relevant data collection and structural refinement parameters are summarized in Table 1. Positional and equivalent displacement parameters are given in Table 2 along with selected interatomic distances in Table 3. The crystallographic information files (CIF) have also been deposited with Fachinformationszentrum Karlsruhe [76344 Eggenstein, Leopoldshafen, Germany; fax: +49 7247 808 666; email: crysdata@fiz.karlsruhe.de; depository numbers CSD-419457 (β-Tb_3Ge_5) and CSD-419458 (β-Dy_3Ge_5)]. Since single crystals of the orthorhombic α-Tb_3Ge_5 polymorph were available for first a time, and since its structure had been established before from powder diffraction work only, we carried out structure refinements based on single-crystal X ray diffraction data The results are not discussed herein, but are in excellent agreement with the earlier Rietveld refinement on the orthorhombic α-Tb_3Ge_5 structure [19] The corresponding CIF has been deposited under CSD-419459.

2.3. Magnetic measurements

Field-cooled dc magnetization (M) measurements were completed for both compounds using a Quantum Design MPMS SQUID magnetometer. The measurements were taken on single-crystalline samples in the temperature range from 2 K to 350 K and in an applied field (H) of 1000 Oe. The raw magnetization data were corrected for the holder contribution and subsequently converted to molar susceptibility ($\chi_m = M/H$).

3. Results and discussion

3.1. Crystal structure

Only a brief account of the structure of the new hexagonal polymorphs of Tb_3Ge_5 and Dy_3Ge_5 (Pearson's symbol *hP*16) will be given here; for a more comprehensive description and comparison between the structures of the two polymorphs, we refer the reader to the report on similar dimorphism in Sm_3Ge_5 [4].

Table 1
Selected single-crystal collection and refinement parameters for Tb_3Ge_5 and Dy_3Ge_5.

Empirical formula	Tb_3Ge_5	Dy_3Ge_5
Formula weight	839.71	850.45
Space group, Z	$P\bar{6}2c$, 2	
Radiation, λ	Mo Kα, 0.71073 Å	
Temperature	120 K	
Unit-cell parameters		
a (Å)	6.861(2)	6.8387(10)
c (Å)	8.339(6)	8.293(2)
V (Å^3)	340.0(3)	335.90(12)
Crystal size	40 μm × 40 μm × 30 μm	50 μm × 40 μm × 40 μm
ρ_{calc} (g/cm^3)	8.203	8.408
μ (cm^{-1})	524.16	548.38
Data/parameter	262/18	261/18
absorption correction method	Semi-empirical, based on equivalents	
Final $R1^a$ ($I > 2\sigma_I$)	$R1$ = 0.0193, $wR2$ = 0.0388	$R1$ = 0.0195, $wR2$ = 0.0469
Final $wR2^b$ ($I > 2\sigma_I$)	$R1$ = 0.0258, $wR2$ = 0.0419	$R1$ = 0.0265, $wR2$ = 0.0510
Largest peak/hole	0.89/−1.20e$^-$/Å^3	0.80/−1.29e$^-$/Å^3

[a] $R1 = \sum ||F_o| - |F_c|| / \sum |F_o|$.
[b] $wR2 = [\sum[w(F_o^2 - F_c^2)^2] / \sum[w(F_o^2)^2]]^{1/2}$, where $w = 1/[\sigma^2 F_o^2 + (A \cdot P)^2 + B \cdot P]$, $P = (F_o^2 + 2F_c^2)/3$; A and B: weight coefficients.

A schematic representation of the structure of β-Tb_3Ge_5 and β-Dy_3Ge_5 is shown in Fig. 1. Using the already communicated ideas [4], this arrangement can be regarded as a long-range ordered superstructure of the non-stoichiometric $TbGe_{2-x}$ and $DyGe_{2-x}$ phases ($x \approx 1/3$) [3]. The relationship between the defect AlB_2 type and the structure in question is straightforward—the periodic array of planar Ge atoms shown in Fig. 2 represents the topology of the $^2_\infty[Ge_5]$-layers in β-RE_3Ge_5, where every 6th atom from the honeycomb-like arrangement in the idealized RE_3Ge_6 (AlB_2 type, formula tripled for convenience) is vacated in a regular fashion. The resultant super-structure, a', will be related to the unit cell of the sub-structure via the simple geometric relationship $a' \approx a \times 3^{1/2}$. In addition, since the newly formed layers are not eclipsed as in the AlB_2-structure, but rather staggered, the c-edge doubles ($c' \approx c \times 2$), yielding an overall 6-fold increase of the cell-volume. Similar approach can be used towards rationalizing the structure of the α-polymorphs (Pearson's code *oF*64), which in turn can be derived from the α-$ThSi_2$ type through ordering of Ge vacancies. In this case, the defect Ge-network can be seen as an array of orthogonal zig-zag chains, $^1_\infty[Ge_2]$, which are interconnected. The imaginary removal of every 6th atom from the chains can result in a three-dimensional lattice (a', b', c') related to its tetragonal "parent" via the relationships: $a' \approx a \times 2^{1/2}$;

Table 2
Atomic coordinates, isotropic displacement parameters (U_{eq}^a) for Tb_3Ge_5 and Dy_3Ge_5.

Atom	Wyckoff index	x	y	z	U_{eq} (Å^2)
		Tb_3Ge_5			
Tb1	6*g*	0.3314(1)	0	0	0.0085(2)
Ge1	6*h*	0.4007(3)	0.3317(3)	1/4	0.0109(3)
Ge2	2*d*	1/3	2/3	1/4	0.0095(6)
Ge3	2*b*	0	0	1/4	0.0104(6)
		Dy_3Ge_5			
Dy1	6*g*	0.33144(9)	0	0	0.0073(2)
Ge1	6*h*	0.4015(3)	0.3314(3)	1/4	0.0124(4)
Ge2	2*d*	1/3	2/3	1/4	0.0098(6)
Ge3	2*b*	0	0	1/4	0.0111(6)

Table 3
Selected interatomic distances (Å) in Tb_3Ge_5 and Dy_3Ge_5.

Atom pair		Distance
	Tb_3Ge_5	
Ge1–	Ge3	2.545(2)
	Ge2	2.561(2)
	Tb × 2	2.945(2)
	Tb × 2	2.970(2)
	Tb × 2	3.450(2)
Ge2–	Ge1 × 3	2.561(2)
	Tb × 6	3.100(5)
Ge3–	Ge1 × 3	2.546(2)
	Tb × 6	3.085(2)
Tb–	Ge1 × 2	2.945(2)
	Ge1 × 2	2.970(2)
	Ge3 × 2	3.085(2)
	Ge2 × 2	3.100(5)
	Ge1 × 2	3.450(2)
	Dy_3Ge_5	
Ge1–	Ge3	2.540(2)
	Ge2	2.558(2)
	Dy × 2	2.929(1)
	Dy × 2	2.956(2)
	Dy × 2	3.441(2)
Ge2–	Ge1 × 3	2.558(2)
	Dy × 6	3.086(2)
Ge3–	Ge1 × 3	2.540(2)
	Dy × 6	3.072(2)
Dy	Ge1 × 2	2.929(1)
	Ge1 × 2	2.956(2)
	Ge3 × 2	3.072(2)
	Ge2 × 2	3.086(2)
	Ge1 × 2	3.441(2)

$b' \approx a \times 2^{1/2} \times 3$; $c' \approx c$. More detailed description can be found elsewhere [4,9,10].

From a different standpoint, both "3–5" structures can also be envisioned as built from triangular prisms made of rare-earth metal atoms that share common faces, and which are centered by germanium atoms (Fig. 1 depicts this for β-RE_3Ge_5). Of worthwhile mention is the fact that not all of these prisms are filled, in fact one out of every six is empty, but this does not cause any distortions in the rare-earth metal sub-lattice.

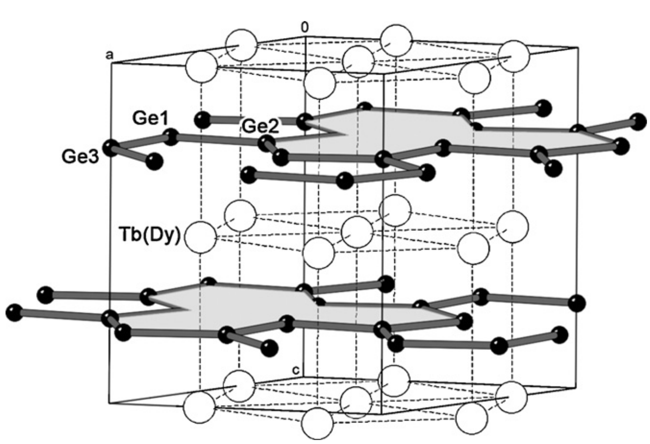

Fig. 1. (a) Crystal structure of the hexagonal β-Tb_3Ge_5 and β-Dy_3Ge_5, viewed down the [1 1 0] plane and with the unit cell outlined. The rare-earth metal atoms are shown as white spheres while Ge atoms are depicted as smaller, black spheres. The 12-membered polygons of Ge, which are the result of the long-range order of vacant Ge sites are shaded. The trigonal prisms formed by the rare-earth metal atoms are drawn with dotted lines.

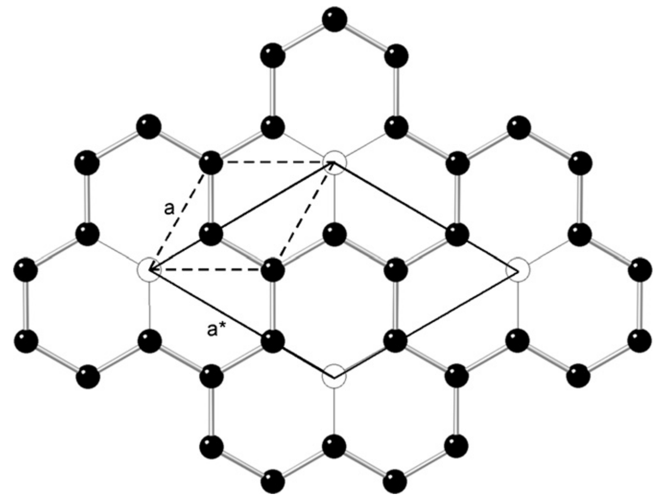

Fig. 2. Schematic representation of the long-range vacancy order in the honeycomb-like layers of Ge in the hexagonal β-Tb_3Ge_5 and β-Dy_3Ge_5. The corresponding subcell-supercell interrelation is also illustrated by dotted and solid lines, respectively.

As discussed in an earlier study [4], there are several key indications, which suggest that the chemical bonding in the non-stoichiometric $TbGe_{2-x}$ and $DyGe_{2-x}$ phases ($x \approx 1/3$) cannot be accurately explained using the AlB_2-type as a model. The first and most significant one has something to do with the fact that the Ge atoms are in special positions in the AlB_2-type (Wyckoff index 2*d*), and have no variable parameters [3]. Thus, the Ge–Ge distances will be interrelated by the lattice constants only, which if the published lattice constants for $TbGe_{2-x}$ and $DyGe_{2-x}$ are taken into consideration [3], amounts to unrealistically short Ge–Ge contacts (on the order of 2.2–2.3 Å). In the 6-fold superstructure (Fig. 2), due to the small distortion around the vacant site in order to compensate for the empty space, the Ge–Ge distances become normal and measure from 2.545(2) Å to 2.561(2) Å in β-Tb_3Ge_5 and 2.540(2) Å to 2.558(2) Å in β-Dy_3Ge_5 (Table 3), along with the Ge–Ge–Ge bonds angles decreasing from 120° to *ca.* 103°. Although these parameters are slightly different than those found in elemental Ge [24], they are comparable to the ones in the recently reported binary germanides such as RE_3Ge_4 (*RE* = Gd through Tm) [6], RE_3Ge_5 (*RE* = Sm, Gd) [4], $EuGe_2$ [17] and $CaGe_2$ [18]. Ultimately, the *RE*–Ge contacts (in which the rare-earth metal is surrounded by 10 next nearest germanium neighbors) are comparable to those found in the latter compounds and measure between *ca.* 2.92 Å and 3.45 Å. A comparison of the *RE*–Ge distances for the known RE_3Ge_5 compounds with this structure shows a good correlation with the decreasing size of the rare-earth metal cations when moving across the lanthanide series. The Ge–Ge distances, however, are invariant upon changing the *RE* metal.

3.2. Phase relationships and structural transformations

It has been known for some time that the binary germanides around 50–67 at.% Ge show large stoichiometry breadths and are often described as $REGe_{2-x}$ ($0 \le x \le 0.5$) [3,9,10]. For the early rare-earth metals, the prevailing structure type is the tetragonal α-$ThSi_2$ (Pearson's symbol *tI*12), while for the mid-to-late rare-earth metals, the layered hexagonal AlB_2 type (Pearson's symbol *hP*3) is more common [1–3]. We have already examined several such $REGe_{2-x}$ phases ($x \approx 1/4$, $x \approx 1/3$, and $x \approx 1/5$), all of which show evidence for superstructures derived from either α-$ThSi_2$ or AlB_2 types through ordering of vacant Ge sites [4–6]. Some of these "line compounds" are not indicated in the corresponding phase diagrams [25], hinting at the possibility that their interpretation may not be as trivial as it may seem at a first glance. Even more surprising is the fact that polymorphic forms and phase transitions are also absent or misrepresented in the diagrams. Take for example the Tb–Ge system [25]—it indicates the possible existence of polymorphic $TbGe_{2-x}$ binaries with compositions $TbGe_{1.6-1.7}$ (62–63 at.% Ge) and $TbGe_{1.5}$ (60 at.% Ge). The structures of the low-temperature forms (LT) remain elusive; the high-temperature form (HT) of $TbGe_{1.6-1.7}$ is with the α-$ThSi_2$ and the latter with the AlB_2 type. The Dy–Ge system [25], in turn, suggests the possible existence of three polymorphic forms of $DyGe_{1.5}$ (type AlB_2 for LT) and only one $DyGe_{1.63}$ (structure unknown). It disagrees with a 1966 paper [26], which describes, perhaps erroneously, two $DyGe_{2-x}$ polymorphs with the α-$ThSi_2$ and AlB_2 type. Several structural studies have subsequently shown that the most thermodynamically stable phases in both diagrams at around 63 at.% Ge are indeed Tb_3Ge_5 and Dy_3Ge_5 (ordered α-$ThSi_2$ superstructures, crystallizing in the *Fdd*2 space group) [19,20]. These compounds have been prepared by direct fusion of the elements and subsequent annealing at between 800 °C and 1000 °C. Such findings are corroborated by our results using the flux growth technique–the formation of the orthorhombic polymorph is facilitated by slow cooling and/or annealing at intermediate temperatures (500–700 °C), whereas the hexagonal form, which is believed to be the metastable (kinetic) phase can be "trapped" when using fast cooling rates only. Another, even more definitive evidence for the α–β phase relationship is the fact that single crystals of the hexagonal phase (β), when annealed in vacuum at temperatures between 500 °C and 700 °C for one week, undergo single-crystal to single-crystal phase transition to the orthorhombic form. This transformation was confirmed by X-ray diffraction (see Section 2) and it appears to be irreversible—annealing of the orthorhombic phase in a large temperature range (from 320 °C to 1000 °C), as detailed in previous studies, does not result in any structural change. The results are fully consistent with the α–β phase relationships reported for Dy_3Ge_5 [20].

3.3. Magnetic properties

Plots of the magnetic susceptibility $\chi = M/H$ as a function of the temperature for both β-Tb_3Ge_5 and β-Dy_3Ge_5 are shown in Fig. 3. As seen from the figure, the two compounds exhibit paramagnetic behavior in wide temperature intervals, according to the Curie–Weiss law: $\chi(T) = C/(T - \theta_p)$, where $C = NA\mu_{eff}^2/3k_B$ is the Curie constant and θ_p is the Weiss temperature (μ_{eff} is the experimental effective moment (in Bohr-magneton units, μ_B) N_A is the Avogadro number (6.022×10^{23} mol^{-1}), k_B is the Boltzmann's constant (1.381×10^{-23} J K^{-1}). Above *ca.* 50 K, the dependence of the inverse susceptibility with the temperature is linear. Applying a linear fit to $\chi^{-1}(T)$ yields effective moments of 9.63 μ_B and 10.47 μ_B for Tb_3Ge_5 and Dy_3Ge_5, respectively. These values are in very good agreement with the values calculated for free-ion Tb^{3+} and Dy^{3+} according to $\mu_{eff} = g[J(J+1)]^{1/2}$ [27]. For both compounds, cusp-like features at temperature of 23 K for Tb_3Ge_5 and 9 K for Dy_3Ge_5 indicate the onset of long-range magnetic order. The magnetic order is probably not simple. The maxima in the $\chi(T)$ plots can be thought as the respective Néel temperatures, and the Weiss temperatures θ_p for Tb_3Ge_5 and Dy_3Ge_5 are both negative: −34 K and −27 K, respectively.

It is worth comparing the magnetic properties of the title compound with those, published for other Tb–Ge and Dy–Ge binaries. For example, $TbGe_2$ (presumed to be a stoichiometric compound) [28] and Tb_3Ge_5 (orthorhombic polymorph) [20] are both antiferromagnetic with Néel temperatures T_N = 42 K and 17 K, respectively. $DyGe_2$ and the orthorhombic Dy_3Ge_5 also undergo antiferromagnetic ordering at 28 K and 12 K, respectively [20]. The difference in the T_N values in both cases could indicate that increasing the concentration of Ge vacancies leads to lowering of the corresponding Néel temperature. Of special mention also is the magnetic order in the Dy–Ge compounds described by Sekizawa [26]. This work reports a HT phase with the α-$ThSi_2$ type and a LT form with the AlB_2 type, which have Néel temperatures of 6.5 K and 23 K, respectively. These data are inconsistent with the neutron diffraction data on the orthorhombic α-Dy_3Ge_5 (LT form) [20] and the discussed herein results on the hexagonal β-polymorph. Such disagreements with earlier studies are not uncommon in the literature, and are most likely due to unrecognized impurities or the presence of secondary phases. After all, the complexity of the corresponding phase diagrams [25] is such that high-quality samples with desired compositions are very difficult to obtain.

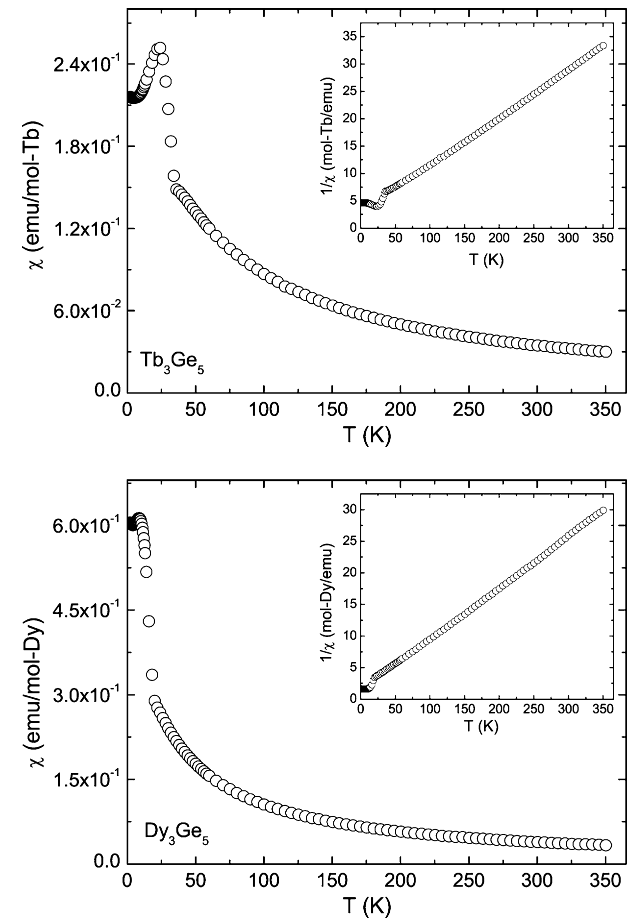

Fig. 3. Temperature dependence of the magnetic susceptibility (χ) plots for β-Tb_3Ge_5 and β-Dy_3Ge_5. Inverse magnetic susceptibility $\chi^{-1}(T)$ plots are shown in the insets.

4. Conclusion

We have reported the synthesis and single-crystal structures of new polymorphs of Tb_3Ge_5 and Dy_3Ge_5. The crystals have successfully been grown from a flux, emphasizing the benefit of the flux-growth method for discovery and facile preparation of single-crystalline compounds. β-Tb_3Ge_5 and β-Dy_3Ge_5 crystallize with hexagonal structures, which are derivatives of the AlB_2 type. The results from these studies are consistent with the earlier reports on polymorphism in Sm_3Ge_5, which all suggest that the hexagonal forms (AlB_2 superstructures, space group $P\bar{6}2c$) are the metastable phases, while the more thermodynamically stable phases in the three *RE*–Ge systems (*RE* = Sm, Tb, Dy) are the orthorhombic RE_3Ge_5 (α-$ThSi_2$ superstructures, space group *Fdd*2). Temperature dependent magnetization measurements show that β-Tb_3Ge_5 and β-Dy_3Ge_5 order antiferromagnetically below 23 K and 9 K, respectively.

Acknowledgements

Svilen Bobev acknowledges financial support from the National Science Foundation through a grant DMR-0743916 (CAREER). PHT wishes to thank the University of Delaware for the University Graduate Fellowship and the International Centre for Diffraction Data (ICDD) for the Ludo Frevel Crystallography Scholarship. Work at Los Alamos was performed under the auspices of the US Department of Energy, Office of Science.

References

[1] A. Szytula, J. Leciejewicz (Eds.), Handbook of Crystal Structures and Magnetic Properties of Rare Earth Intermetallics, CRC Press, Boca Raton, FL, 1994.
[2] A. Iandelli, A. Palenzona, in: K.A. Gschneidner Jr., L. Eyring (Eds.), Handbook on the Physics and Chemistry of Rare Earths, vol. 2, North Holland, Amsterdam, 1979, p. 1.
[3] P. Villars, L.D. Calvert, Pearson's Handbook of Crystallographic Data for Intermetallic Phases, second ed., American Society for Metals, Materials Park, OH, 1991.
[4] P.H. Tobash, D. Lins, S. Bobev, N. Hur, J.D. Thompson, J.L. Sarrao, Inorg. Chem. 45 (2006) 7286.
[5] P.H. Tobash, S. Bobev, W. Pryz, D. Buttrey, N. Hur, J.D. Thompson, J.L. Sarrao, in preparation.
[6] P.H. Tobash, G. DiFilippo, S. Bobev, N. Hur, J.D. Thompson, J.L. Sarrao, Inorg. Chem. 46 (2007) 8690.
[7] G. Venturini, I. Ijjaali, B. Malaman, J. Alloys Compd. 289 (1999) 168.
[8] A.M. Guloy, J.D. Corbett, Inorg. Chem. 30 (1991) 4789.
[9] G. Venturini, I. Ijjaali, B. Malaman, J. Alloys Compd. 284 (1999) 262.
[10] G. Venturini, I. Ijjaali, B. Malaman, J. Alloys Compd. 285 (1999) 194.
[11] G. Venturini, I. Ijjaali, B. Malaman, J. Alloys Compd. 289 (1999) 116.
[12] O. Zaharko, P. Schobinger-Papamantellos, C. Ritter, J. Alloys Compd. 280 (1998) 4.
[13] M.G. Kanatzidis, R. Pöttgen, W. Jeitschko, Angew. Chem. Int. Ed. 44 (2005) 6996.
[14] P.H. Tobash, D. Lins, S. Bobev, A. Lima, M.F. Hundley, J.D. Thompson, J.L. Sarrao, Chem. Mater. 17 (2005) 5567.
[15] P.H. Tobash, S. Bobev, J. Am. Chem. Soc. 128 (2006) 3532.
[16] P.H. Tobash, J.J. Meyers, G. DiFilippo, S. Bobev, F. Ronning, J.D. Thompson, J.L. Sarrao, Chem. Mater. 20 (2008) 2151.
[17] S. Bobev, E.D. Bauer, J.D. Thompson, J.L. Sarrao, G.J. Miller, B. Eck, R. Dronskowski, J. Solid State Chem. 177 (2004) 3545.
[18] P.H. Tobash, S. Bobev, J. Solid State Chem. 180 (2007) 1575.
[19] P. Schobinger-Papamantellos, K.H.J. Buschow, J. Less-Common Met. 146 (1989) 279.
[20] P. Schobinger-Papamantellos, D.B. de Mooij, K.H.J. Buschow, J. Less-Common Met. 163 (1990) 319.
[21] JADE Version 6.5, Materials Data, Inc., Livermore, CA, 2003.
[22] SAINT NT, Version 6.45, Bruker Analytical X-Ray Systems, Inc., Madison, WI, 2003.
[23] SADABS NT, version 2.10, Bruker Analytical X-Ray Systems, Inc., Madison, WI, 2001.
[24] L. Pauling, The Nature of the Chemical Bond, third ed., Cornell University Press, Ithaca, NY, 1960.
[25] T.B. Massalski, Binary Alloy Phases Diagrams, American Society for Metals, Materials Park, OH, 1990.
[26] K. Sekizawa, J. Phys. Soc. Jpn. 21 (1966) 1137.
[27] J.S. Smart, Effective Theories of Magnetism, Saunders, Philadelphia, PA, 1966.
[28] P. Schobinger-Papamantellos, D.B. de Mooij, K.H.J. Buschow, J. Less-Common Met. 144 (1988) 265.